

# Photoinduced Interfacial Charging and “Explosion” of Monolayer Pentacene Islands

Liwei Chen,<sup>\*,†</sup> Oksana Cherniavskaya,<sup>‡</sup> Alexander Shalek,<sup>§</sup> and Louis E. Brus

Columbia University, Department of Chemistry, New York, New York 10027

Received August 9, 2005; Revised Manuscript Received September 14, 2005

## ABSTRACT

Electrostatic force microscopy shows that the electric field gradients above pentacene monolayer islands on 2-nm SiO<sub>2</sub>/Si substrates, in a dark, dry nitrogen environment, display a wide distribution of signs and magnitude that is dependent on sample history. Under 12 mW/cm<sup>2</sup> green (532 nm) illumination, pentacene islands accumulate positive charge because of photoexcited electron transfer across the oxide to the Si substrate. At a strong illumination of 60 mW/cm<sup>2</sup>, pentacene islands reform into small spherical particles, apparently because the positive charge Coulomb repulsion energy becomes comparable to the cohesive energy of the pentacene monolayer.

**Introduction.** Organic electronics use films of weakly interacting,  $\pi$ -bonded molecules to construct inexpensive thin-film transistors (TFTs), typically for lightweight and flexible displays.<sup>1–4</sup> Among these, conjugated small molecules such as pentacene and sexithiophene have demonstrated some of the best charge transport properties.<sup>5,6</sup> Organic TFT devices work in the accumulation mode in which current modulation is confined to the interface layer with gate dielectrics.<sup>7</sup> Recent works report that the hole mobility approaches typical organic FET values when the film thickness reaches two monolayers in sexithiophene devices, or six monolayers in pentacene devices.<sup>8,9</sup> The interface is critical; for example, hydroxyl groups at the gate interface introduce electron trap states in polymer TFTs;<sup>10</sup> passivation of hydroxyls on SiO<sub>2</sub> effectively reduces the density of the interfacial trapping states.<sup>11</sup>

We try to understand the kinetic and equilibrium aspects of pentacene charging at this interface. Scanning probe methods have been used to study the microscopic electronic origin of device parameters observed in transport measurements. Using electrostatic force microscopy (EFM), Marohn et al. found that hole traps exist within pentacene grains as well as at grain boundaries in an operating pentacene TFT device.<sup>12</sup> The Vuillaume group studied electron and hole injection from an AFM tip into pentacene monolayer islands.<sup>13</sup> Previously, we observed a substantial interface dipole at the monolayer island pentacene/SiO<sub>2</sub> interface in

UHV on thick oxides and pentacene induced gap states on thin oxides.<sup>14</sup> We now report pentacene laser photoionization on thin (~2 nm) thermal oxides, where electronic equilibrium with the underlying silicon is possible. This allows us to drive the system far from equilibrium so that the resulting relaxation kinetics might be followed. Here, we report photoinduced charging behavior under nitrogen atmosphere as a function of prior ambient exposure.

**Experimental Section.** Monolayer islands of pentacene (1.8 ± 0.2 nm) were deposited via thermal evaporation in high vacuum on degenerately doped n-type Si (Sb-doped, 0.008–0.03 Ω cm) and p-type Si (B-doped, 0.005–0.01 Ω cm) substrates with a 2-nm thermally grown oxide layer (IBM Research, Yorktown Heights, NY) using a procedure described previously.<sup>14</sup> After deposition, samples were exposed to ambient atmosphere for about 2 h. Electrostatic force microscopy (EFM) images were taken using a Digital Instruments Nanoscope IIIa MultiMode AFM (Santa Barbara, CA) in a dry nitrogen box (MBruan Inc., Stratham, NH, moisture and oxygen level less than 1 ppm). For each image line, a normal tapping mode AFM scan without applied voltage was first performed to obtain the sample topography. This was followed by an EFM line scan in which the tip was lifted to a constant height,  $Z_{\text{lift}}$ , of 10 nm above the sample surface, while a bias voltage  $V = V_{\text{dc}} + V_{\text{ac}} \sin(\omega t)$  was applied.<sup>15</sup> Typically, a  $V_{\text{dc}}$  value between –0.1 and –0.3 V is used to balance the surface potential difference between the tip and the SiO<sub>2</sub> substrate, and a  $V_{\text{ac}}$  of 3 V is applied to ensure strong EFM signals. Pt–Ir coated EFM tips (nanosensor EFM20) from Molecular Imaging (Phoenix, AZ) with resonance frequencies around 65 kHz were used. EFM probe spring constants were measured to be around 1.2 N/m.<sup>16</sup> The

\* Corresponding author. E-mail: lwchen@helios.phy.ohio.edu.

† Current address: Ohio University, Department of Chemistry and Biochemistry, Athens, OH 45701.

‡ Current address: Columbia University, Department of Biological Sciences, New York, NY 10027.

§ Current address: Harvard University, Department of Chemistry and Chemical Biology, Cambridge, MA 02138.

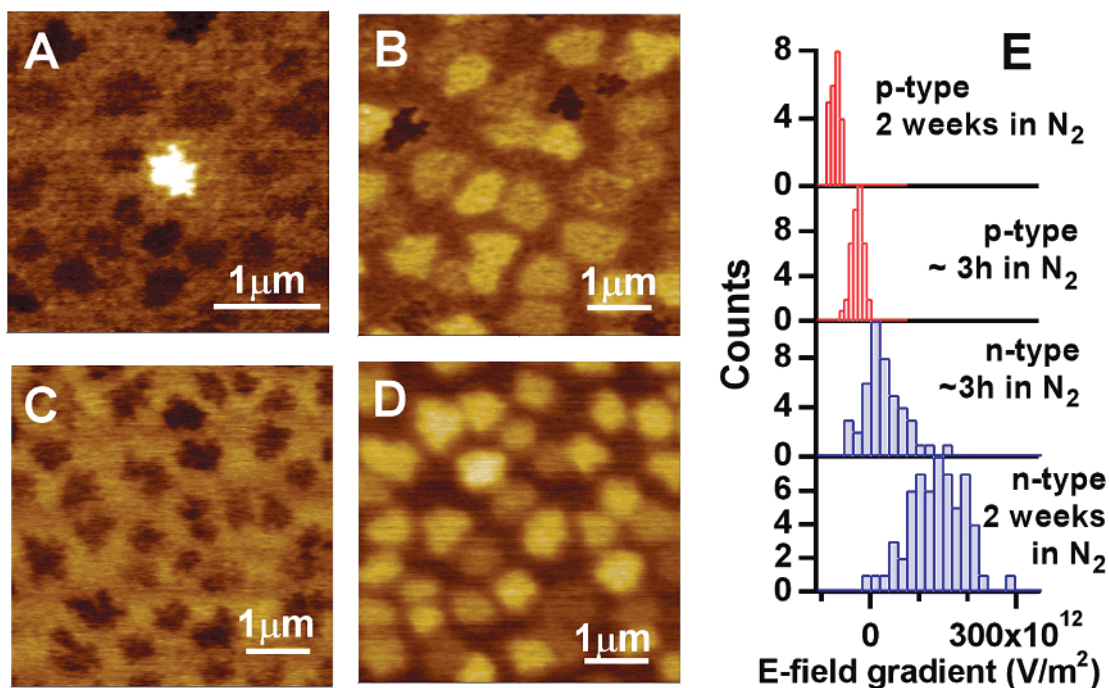


**Figure 1.** (A–D) Electric field gradient images of pentacene monolayer islands on Si substrates with 2-nm thermal oxide in the dark. The height of the islands is  $1.8 \pm 0.2$  nm. (A and C): p-type Si substrate; (B and D): n-type Si substrate. (E) Sample history dependence of the E-field gradient statistics. All samples were exposed to the ambient for  $\sim 2$  h prior to storage in a dry nitrogen box.

capacitance of each individual tip with the substrate was calibrated as described previously.<sup>15</sup> Overall, these measurements allowed us to convert measured force gradients to absolute charge on the films accurately, as explained in the Supporting Information. Samples were photoexcited with a 20-mW 532-nm CW laser (Information Unlimited, Amherst, NH, Model no. LM532P20) at grazing angle incidence. Scanning Kelvin Probe Microscopy (SKPM) was performed with the DI software package, and the surface potential measurements were cross-checked by the  $V_{dc}$  bias voltage that zeros the EFM signal. SKPM differs from EFM in that feedback is applied to the tip bias after the force gradient is measured.

**Results. In the Dark.** Pentacene absorbs visible light. With ambient light blocked, most as-deposited pentacene islands on a p-type Si substrate (Figure 1A and C) show a static electric field above their surface corresponding to a negative charge or an electric dipole with the negative end pointing toward the tip. There are a few exceptions that show the opposite (Figure 1A). However, most pentacene islands on n-type substrates show positive charges (Figure 1B and D). The E-field gradients above the pentacene islands on both p- and n-type Si have broad distributions. Less than 3% of islands show electric fields opposite to the majority depending on the sample history. Figure 1E shows that for the samples that had been exposed to air for  $\sim 2$  h and then stored in a dry nitrogen box for ca. 3 h the E-field gradient is relatively weak and close to neutral. The signal becomes stronger after two weeks in nitrogen with samples on p-type substrates acquiring more negative charge, and the samples on n-type substrates acquiring more positive charge. After two weeks in the dry nitrogen box, all islands on a given sample show the same sign charge. The measured force

gradients shown in Figure 1 correspond to E-field gradients on the order of  $10^{14}$  V/m<sup>2</sup> (Supporting Information), using an EFM tip having a capacitance of ca.  $3 \times 10^{-18}$  F when lifted  $\sim 10$  nm above the substrate.<sup>15</sup>

The band alignment at the SiO<sub>2</sub>/pentacene interface in the nitrogen environment is measured using SKPM. The surface potential of the pentacene islands is 0.1 V higher than that of the SiO<sub>2</sub> background on n-type substrates, but 0.05 V lower on p-type substrates. The surface potential variation among islands in the dark is much less than 0.1 eV, and thus does not change the band alignment significantly.

**Moderate Illumination.** Under ca. 12 mW/cm<sup>2</sup> green illumination, the E-field gradient signal above pentacene islands on both n- and p-type substrates shifts up (Figure 2), indicating an accumulation of positive charge. The pentacene islands that are negatively charged on p-type substrates (Figure 2A) become nearly neutral upon illumination, with a few islands becoming slightly positive (Figure 2B). The islands that are positively charged in the dark on n-type substrates (Figure 2C) become more positive (Figure 2D). Figure 2F shows the time evolution of an EFM signal averaged over five islands during an excitation and relaxation cycle. Both the rise and the decay can be fit with single exponentials for samples on both n- and p-type substrates. For the sample on an n-type substrate, rise and decay time constants of 28 and 34 min are obtained. On the p-type substrates, we obtained rise and decay time constants of 35 and 37 min, respectively. After about 2 h, the EFM signal decays back to the same level as before illumination in both samples. Thus, under laser illumination a photostationary charged state is achieved. At this intensity, we observed experimentally that slightly increasing the laser intensity leads to a higher photostationary positive charge.

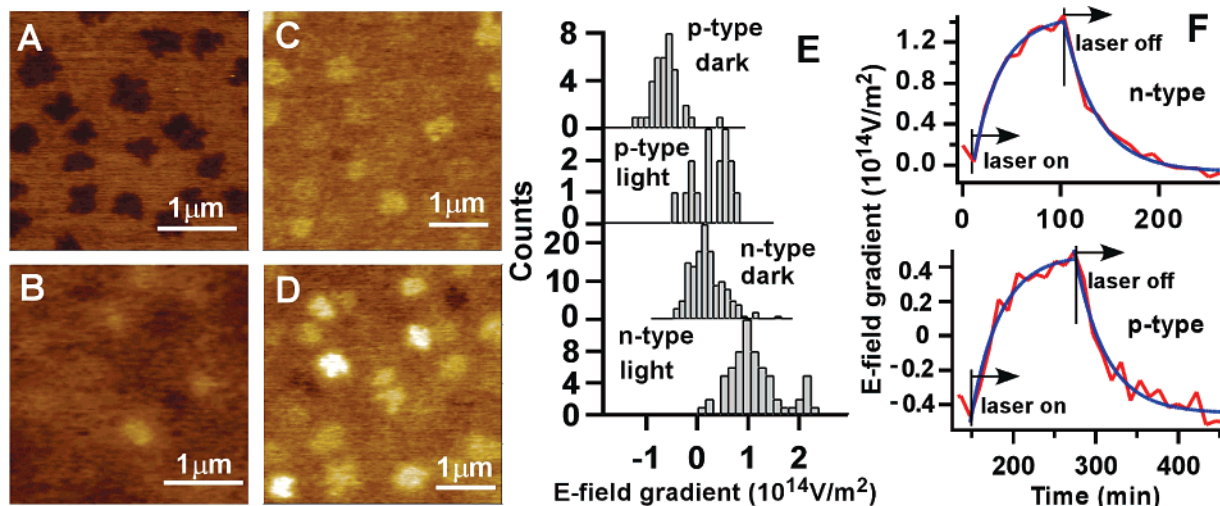


**Figure 2.** Photoinduced charging of pentacene monolayer islands at 532 nm. (A and C): EFM images in the dark; (B and D): EFM images with the laser on ( $12 \text{ mW/cm}^2$ ). (A and B): pentacene on p-type Si substrate; (C and D): pentacene on n-type substrate. (E) Histograms of E-field gradient above pentacene islands in the dark and under steady-state 532-nm illumination. (F) Red traces: average time trajectory of the E-field gradient on five islands when the laser is turned on and off. Blue traces: single-exponential fit of the average time trajectory.

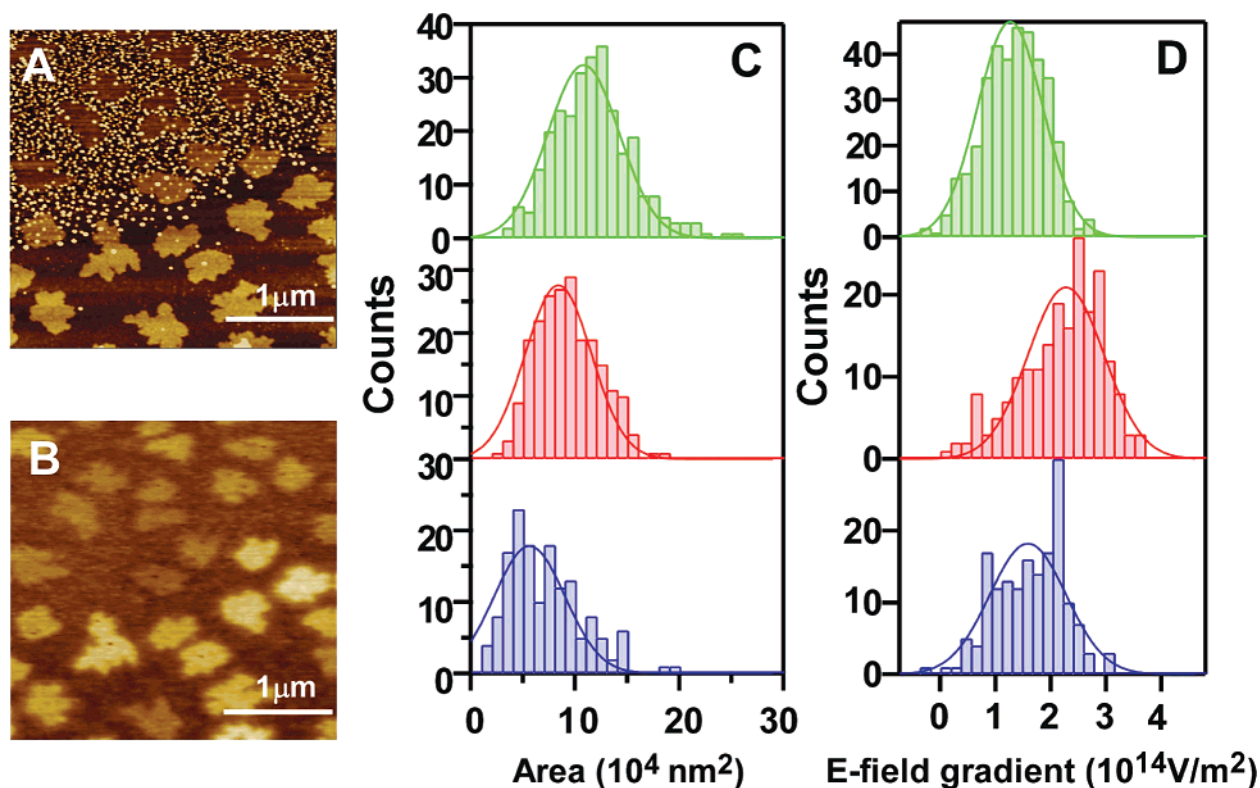


**Figure 3.** (A) Topography and (B) E-field gradient images of pentacene monolayer islands on n-type Si after  $60 \text{ mW/cm}^2$  illumination at 532 nm. Statistical distribution of island size and E-field are shown in C and D, respectively. Green: distribution of the sample in the dark; red: distribution after strong illumination in areas without the spherical particles; blue: distribution after strong illumination in areas with spherical particles.

*Stronger Illumination.* Drastically different behavior, a change in topography, is observed upon  $\sim 60 \text{ mW/cm}^2$  illumination of samples on n-type substrates, where, as discussed above, the residual charge in the dark is initially positive. At this intensity, an order-of-magnitude estimate indicates that each pentacene molecule is excited  $\sim 4$  times per second. The topography image (Figure 3A) shows circular regions ( $\sim 10 \mu\text{m}$  in diameter) with many small

spherical particles 5–8 nm in height. These round particles are created by illumination. There are also a few of these round spherical particles in the area surrounding the circular regions. Spherical particles are not seen in samples on p-type substrates whose charge is initially negative. The particles appear during the first scan (less than five minutes) after the CW laser is turned on, and remain after the laser is turned off. In the circular regions with many particles, the remaining



pentacene islands are smaller,  $(5.6 \pm 3) \times 10^4 \text{ nm}^2$  in area as compared with  $(11 \pm 3) \times 10^4 \text{ nm}^2$  (Figure 3C) before illumination. We tentatively conclude that round pentacene particles have been formed from molecules initially in the monolayer islands. The pentacene islands before illumination generate a relatively high EFM signal of  $(1.2 \pm 0.6) \times 10^{14} \text{ V/m}^2$ . Under the strong laser light, the surrounding region with few spherical particles accumulated high charge that caused an EFM signal of  $(2.3 \pm 0.6) \times 10^{14} \text{ V/m}^2$ . However, in the circular region with the particles, the E-field gradient on pentacene islands is only  $(1.7 \pm 0.6) \times 10^{14} \text{ V/m}^2$  (Figure 3B and D).

**Discussion. In the Dark.** The electric force gradient above pentacene islands in the dark is typically on the order of  $10^{-4} \text{ N/m}$ . If the pentacene islands are modeled as 1.8-nm-thick disks 300 nm in diameter with a uniform dipole density that extends from the pentacene/SiO<sub>2</sub> interface to the mid-height of the pentacene disk, then an E-force gradient of  $5 \times 10^{-4} \text{ N/m}$  at the 10-nm lift height would require a dipole density of  $1 \times 10^{18} \text{ D/m}^2$  or 0.24 D/molecule. This dipole density corresponds to  $5.5 \times 10^{-3}$  elementary charges separated by 9 Å across the molecular axis. Alternatively, if the  $5 \times 10^{-4} \text{ N/m}$  E-force gradient were to originate from pure charge with its partial image charges in the substrate (as described in the Supporting Information), then a uniform charge density of  $0.0024 \text{ C/m}^2$  located 0.9 nm above the SiO<sub>2</sub> surface across the disk is necessary. This corresponds to  $3.6 \times 10^{-3}$  positive elementary charges per molecule, or, a total of about 1000 positive charges in the 300-nm-diameter pentacene disk (Supporting Information). This dark, background charge density is higher than the recently reported  $1.3 \times 10^{-4} \text{ e/molecule}$  “remnant charge” on pentacene islands on 4-nm-thick SiO<sub>2</sub>, but lower than that on Si substrates with native oxide ( $1.1 \times 10^{-2} \text{ e/molecule}$ ).<sup>13</sup>

These initial dark electric field gradients depend on gas exposure. The majority of pentacene islands on both p- and n-type substrates imaged here give E-field directions opposite of those of similar samples (on the same batch of substrates) that we imaged previously in UHV.<sup>14</sup> Pentacene on n-type silicon imaged in UHV displays a negative E-field gradient; after 2 h of exposure to ambient during sample transfer, the same sample shows neutral to slightly positive E-field gradient in the dry nitrogen box. The difference between UHV and nitrogen, and the slow drifting of the E-field signal in dry nitrogen (Figure 1E) may result from slow charge transfer related to trace oxygen or water physically trapped in the pentacene. In this context, note that “dry nitrogen” in principle may still have milliTorr levels of oxygen and water vapor. Previous EFM measurements on carbon nanotubes adsorbed on Au surfaces showed contact potential differences and net charges that were strongly sensitive to exposure to the atmosphere.<sup>17</sup>

The variability of pentacene charge on a given substrate may be partially due to nearby random positive and negative fixed charge in the oxide.<sup>18,19</sup> These static charges give rise to heterogeneous local fields and have been shown to polarize spin-coated nanoparticles.<sup>20</sup>

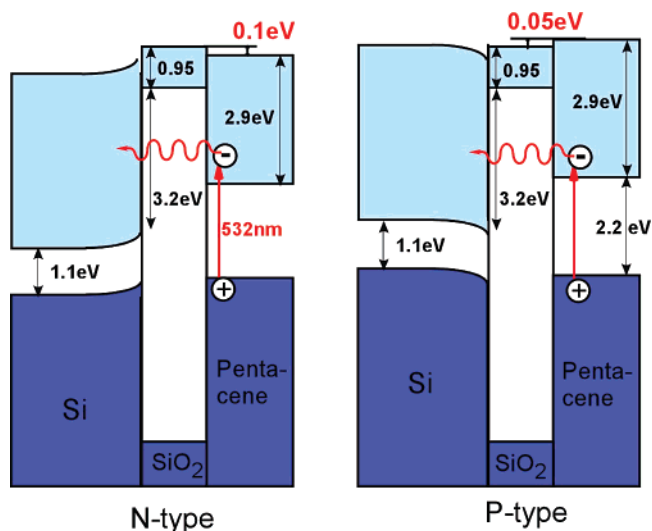


**Figure 4.** Illustration the pentacene/SiO<sub>2</sub> interface energy band alignment in nitrogen and the mechanism of pentacene monolayer charging.

**Moderate Illumination.** The EFM measurements shown in Figure 2 indicate that the pentacene film accumulates a positive charge upon illumination at 532 nm. After the laser is turned off, the EFM signal decays back to original levels. This suggests a reversible charging and discharging process. The photon energy of the 532-nm light is 2.3 eV, greater than the 2.2 eV band gap of pentacene thin film. The simplest explanation is that electrons tunnel to the Si substrate from the optically created excited electronic state of pentacene. The band diagram at the interface based on the surface potential measured in a nitrogen box is shown in Figure 4. The 532-nm light excites electrons to the pentacene conduction band and leaves holes in the valence band. The electrons in the conduction band have a higher probability of tunneling across the oxide barrier to the Si because there are empty states in the Si conduction band at the same energy. However, the hole states at the valence band maximum roughly align with the top of the valence band of the n-type Si substrate, about 0.15 eV above the top of the p-type Si valence band; therefore, the density of states available in Si for holes to tunnel is much smaller than that for electrons. A previous study of CdSe/CdS core–shell nanocrystal optical excitation using the same 2-nm oxide substrates used in this study also showed positive photocharging, with similar rise and decay times on the time scale of 1 h.<sup>21,22</sup> With pentacene, however, we do not observe the strong difference in rates between n and p substrates that was seen previously for the nanocrystals.

**Strong Illumination.** The pentacene island size distribution (Figure 3C) reveals that the average island size is reduced when small spherical particles are produced. This suggests that pentacene partially reforms into particles. The small particles only appear when n-type samples that originally bear strong positive E-force gradient signals ( $\sim 1.2 \times 10^{-3} \text{ N/m}$ ) in the dark are illuminated with a strong laser light. Photogeneration of particles results from highly charged pentacene islands. Indeed, the nearby sample regions (with fewer particles) have an average of  $2.3 \times 10^{-3} \text{ N/m}$  E-force gradient on pentacene islands after illumination, which is

the highest value seen among all of the samples and all of the conditions in this study. This corresponds to a charge density level of  $2 \times 10^{-2}$  positive charges/molecule. These positive charge levels are more than an order of magnitude larger than those created previously by tip charging.<sup>13</sup>

A possible mechanism is Coulombic “explosion” as positive charge continues to increase in a van der Waals bonded monolayer. The cohesive energy of the pentacene monolayer islands is roughly the sublimation enthalpy,  $\sim 184$  kJ/mol at 25 °C.<sup>23</sup> With the lattice unit cell volume of 692 Å<sup>3</sup> each containing two molecules, we calculate the cohesive energy for a 300-nm diameter circular disk of monolayer pentacene to be about  $1 \times 10^{-13}$  J. However, a  $2.3 \times 10^{-3}$  N/m E-force gradient at the disk center corresponds to a charge density of about 0.012C/m<sup>2</sup>, which is equivalent to about 4800 charges distributed evenly in the disk (1 positive charge per 14 nm<sup>2</sup>). The total energy needed to assemble this charge distribution is calculated to be  $1.5 \times 10^{-14}$  J (Supporting Information), about one-sixth of our approximate cohesive energy. This order-of-magnitude estimate suggests that it is possible that further photocharging of the islands may lead to island disintegration.

**Conclusions and Remarks.** The EFM signal on pentacene islands in dry nitrogen shows a wide distribution and strong sample history dependence. This indicates that charging at the pentacene/SiO<sub>2</sub> interface is highly sensitive to the gaseous environment (likely trapped oxygen and moisture) as well as the charge heterogeneity of the substrate. Photocharging of the pentacene islands reveals that electronic equilibrium across the 2-nm thin SiO<sub>2</sub> dielectric layer occurs on a time scale of minutes to hours. This points to the important issue of gate leakage in the scaling down of organic electronic devices. Further, the charge-induced dissociative explosion of the pentacene islands suggests that film stability is a concern in monolayer films of van der Waals bonded organic semiconductors when subjected to high field.

**Acknowledgment.** We thank Alejandro Schrott and Cherie Kagan at IBM Watson Research Center for providing the pentacene monolayer sample. This work has been supported primarily by the Nanoscale Science and Engineer-

ing Initiative of the National Science Foundation under NSF award no. CHE-0117752 and by the New York State Office of Science, Technology, and Academic Research (NYSTAR).

**Supporting Information Available:** Quantitative analysis of the EFM signal strength. This material is available free of charge via the Internet at <http://pubs.acs.org>.

## References

- (1) Forrest, S. R. *Nature* **2004**, *428*, 911–918.
- (2) Rogers, J. A.; Bao, Z.; Katz, H. E.; Dodabalapur, A. In *Thin-Film Transistors*; Marcel Dekker Inc.: New York, 2003; pp 377–425.
- (3) Dimitrakopoulos, C. D.; Malenfant, P. R. L. *Adv. Mater.* **2002**, *14*, 99–117.
- (4) Jackson, N.; Lin, Y. Y.; Gundlach, D. J.; Klauk, H. *IEEE J. Quantum Electron.* **1998**, *4*, 100–104.
- (5) Lin, Y. Y.; Gundlach, D. J.; Nelson, S. F.; Jackson, T. N. *IEEE Electron Device Lett.* **1997**, *18*, 606–608.
- (6) Lin, Y. Y.; Gundlach, D. J.; Nelson, S. F.; Jackson, T. N. *IEEE Trans. Electron Devices* **1997**, *44*, 1325–1331.
- (7) Horowitz, G.; Hajlaoui, R.; Bouchriha, H.; Bourguiga, R.; Hajlaoui, M. *Adv. Mater.* **1998**, *10*, 923–927.
- (8) Dinelli, F.; Murgia, M.; Levy, P.; Cavallini, M.; Biscarini, F.; de Leeuw, D. M. *Phys. Rev. Lett.* **2004**, *92*, 116802.
- (9) Ruiz, R.; Papadimitratos, A.; Mayer, A. C.; Malliaras, G. G. *Adv. Mater.* **2005**, *17*, 1795–1798.
- (10) Chua, L. L.; Zaumseil, J.; Chang, J. F.; Ou, E. C. W.; Ho, P. K. H.; Sirringhaus, H.; Friend, R. H. *Nature* **2005**, *434*, 194–199.
- (11) Yagi, I.; Tsukagoshi, K.; Aoyagi, Y. *Appl. Phys. Lett.* **2005**, *86*, 103502.
- (12) Muller, E. M.; Marohn, J. A. *Adv. Mater.* **2005**, *17*, 1410–1414.
- (13) Heim, T.; Lmimouni, K.; Vuillaume, D. *Nano Lett.* **2004**, *4*, 2145–2150.
- (14) Chen, L. W.; Ludeke, R.; Cui, X. D.; Schrott, A.; Kagan, C. R.; Brus, L. E. *J. Phys. Chem. B* **2005**, *109*, 1834–1838.
- (15) Cherniavskaya, O.; Chen, L. W.; Weng, V.; Yuditsky, L.; Brus, L. E. *J. Phys. Chem. B* **2003**, *107*, 1525–1531.
- (16) Hutter, J. L.; Bechhoefer, J. *Rev. Sci. Instrum.* **1993**, *64*, 1868–1873.
- (17) Cui, X. D.; Freitag, M.; Martel, R.; Brus, L.; Avouris, P. *Nano Lett.* **2003**, *3*, 783–787.
- (18) Ludeke, R.; Cartier, E. *Microelectron. Eng.* **2001**, *59*, 259–263.
- (19) Ludeke, R.; Cartier, E. *Appl. Phys. Lett.* **2001**, *78*, 3998–4000.
- (20) Ben-Porat, C. H.; Cherniavskaya, O.; Brus, L.; Cho, K. S.; Murray, C. B. *J. Phys. Chem. A* **2004**, *108*, 7814–7819.
- (21) Cherniavskaya, O.; Chen, L. W.; Brus, L. *J. Phys. Chem. B* **2004**, *108*, 4946–4961.
- (22) Cherniavskaya, O.; Chen, L. W.; Islam, M. A.; Brus, L. *Nano Lett.* **2003**, *3*, 497–501.
- (23) Dekruif, C. G. *J. Chem. Thermodyn.* **1980**, *12*, 243–248.

NL051567M